Time-Variant Channel Prediction for Interference Alignment with Limited Feedback

Zhinan Xu, Thomas Zemen
FTW (Telecommunications Research Center Vienna)
Vienna, Austria
Email: {xu, thomas.zemen}@ftw.at

***Abstract*—We propose a novel limited feedback algorithm for single-input single-output (SISO) interference alignment in time-variant channels. The feedback algorithm enables reduced-rank channel prediction to compensate for the channel estimation error due to time selectivity and feedback delay. An upper bound for the rate loss caused by feedback quantization and channel prediction is derived. We characterize the scaling of the required number of feedback bits in order to decouple the rate loss due to channel quantization from the transmit power. Based on our derived upper bound, we develop a dimension switching algorithm which is able to find the best tradeoff between quantization error and prediction error. Simulation results show that a rate gain over the traditional non-predictive feedback strategy can be secured and a 60% higher rate is achieved at 20dB signal-to-noise ratio.**

I. Introduction

Interference alignment (IA) is able to achieve the optimal degrees of freedom (DoF) at high signal-to-noise ratios (SNRs) and a rate of $K/2 \cdot \log(\mathrm{SNR}) + o(\log(\mathrm{SNR}))$ for the K user interference channel with time-variant coefficients [1]. However, this result is based on the assumption that *global* channel state information (CSI) is perfectly known at all nodes. This is extremely hard to achieve due to the large amount of required feedback information. Limited CSI feedback [2] is a promising approach to obtain CSI at the transmitter side in frequency division duplex (FDD) systems.

CSI feedback for IA has been investigated in [3], [4], assuming perfect channel estimation. In [3], channel coefficients are quantized using a Grassmannian codebook for frequency-selective single-input single-output (SISO) channels. The work in [4] extends the results to multiple-input multiple-output (MIMO) channels. Both [3] and [4] show that the full DoF are achievable as long as the feedback rate is high enough (which scales with the transmit power). However, for a practical system, the following issues have to be addressed: (a) For time-variant channels, CSI is acquired with the aid of pilots. The channel varies over time due to the mobility of the users. If the channel changes after the transmission of the pilots, the receiver can not detect the variation, which leads to a reduction in sum rate due to the use of outdated channel estimates. (b) For FDD, the CSI is fed back through limited capacity broadcast feedback channels. The error due to quantized feedback degrades the IA performance. (c) The feedback information arrives at the transmitter with a delay which causes a further performance degradation. (d) Overhead, which comes with pilot insertion, does not convey any payload information, leading to a reduction of spectral efficiency.

In this paper, we jointly consider the first three problems and leave (d) for future work. *Contribution of the paper*:

- We tackle the problems (a) and (c) by reduced-rank channel prediction using discrete prolate spheroidal (DPS) sequences [5]. Thanks to the energy concentration of the sequences in the Doppler domain, we are able to describe the channel evolution by a few subspace coefficients.
- To address problem (b), we show that, with a reformulation, the subspace coefficients can be quantized and fed back on a Grassmannian manifold. It greatly reduces the redundancy of the codebook by exploiting the rotation invariance. With the subspace coefficients, the transmitter is able to perform channel prediction to combat the time selectivity of the channel.
- An upper bound of the rate loss due to the channel prediction- and quantization-error is derived.
- We characterize the scaling of the required number of feedback bits in order to decouple the rate loss due to quantization from the transmit power.
- We show that there exists a tradeoff between quantization error and prediction error at a given feedback rate. We develop a subspace dimension switching algorithm to find the best tradeoff such that the sum rate is maximized.

II. System model

Let us consider a K user time- and frequency-selective SISO interference channel, which consists of K transmitter and receiver pairs. The L-tap time-variant impulse response between transmitter j and receiver i is denoted by $\mathbf{h}_{i,j}[t] = \left[h^1_{i,j}[t], \ldots, h^L_{i,j}[t]\right]^{\mathrm{T}}$, $\forall i,j \in \{1,\ldots,K\}$. Every element $h^\ell_{i,j}[t]$ of the channel impulse response is an independent identically distributed (i.i.d.) symmetric complex Gaussian random variable with zero mean and variance $p^\ell_{i,j}$ for $l \in \{1,\ldots,L\}$. Thus, the covariance matrix $\mathbb{E}\{\mathbf{h}_{i,j}[t]\mathbf{h}_{i,j}[t]^{\mathrm{H}}\} = \mathrm{diag}(\left[p^1_{i,j},\ldots,p^L_{i,j}\right])$. We assume $\sum_{l=1}^{L} p^\ell_{i,j} = 1$. The temporal covariance function over consecutive orthogonal frequency division multiplexing (OFDM) symbols $R_{\mathbf{h}_{i,j}}[m] = \mathbb{E}\{\mathbf{h}_{i,j}[t]^{\mathrm{H}}\mathbf{h}_{i,j}[t+m]\} = J_0(2\pi\nu_{\mathrm{D}}m)$ where J_0 is the 0-th order Bessel function of the first kind and $\nu_{\mathrm{D}} = f_{\mathrm{D}}T_{\mathrm{s}}$ denotes the normalized Doppler frequency, where f_{D} denotes the Doppler frequency in Hertz (Hz) and T_{s} denotes the OFDM symbol duration.

We use OFDM to convert the time and frequency selective channel into N parallel time-selective and frequency-flat channels. The $N \times 1$ frequency response is defined as $\mathbf{w}_{i,j}[t] = \mathcal{F}_N\{[\mathbf{h}_{i,j}[t]^{\mathrm{T}}, \mathbf{0}_{1\times(N-L)}]^{\mathrm{T}}\}$, where $\mathcal{F}_N$ denotes the N-point discrete Fourier transform. The diagonal matrix containing the channel frequency response becomes $\mathbf{W}_{i,j}[t] = \mathrm{diag}\left(\mathbf{w}_{i,j}[t]\right)$.

For a given transmitter, its signal is only intended to be received by a single user for a given signaling interval. The signal received at receiver i is the superposition of the signals transmitted by all transmitters, which can be written as

$$\mathbf{y}_i[t] = \mathbf{W}_{i,i}[t]\mathbf{x}_i[t] + \sum_{i\neq j} \mathbf{W}_{i,j}\,[t]\,\mathbf{x}_j[t] + \mathbf{n}_i[t]\,, \qquad (1)$$

where the vector $\mathbf{x}_i[t] \in \mathbb{C}^{N\times 1}$ is the OFDM symbol sent by user i with power constraint $\mathbb{E}\{\mathbf{x}_i[t]^{\mathrm{H}}\mathbf{x}_i[t]\} = PN$, where P is the transmit power per subcarrier. Additive complex symmetric Gaussian noise at receiver i is denoted by $\mathbf{n}_i[t] \sim \mathcal{CN}(0, \sigma^2\mathbf{I}_{N\times 1})$. The SNR is defined as $\mathrm{SNR} = \frac{P}{\sigma^2}$.

In this work we consider a user velocity and carrier frequency such that the Doppler bandwidth of the fading process f_D is much smaller than the subcarrier spacing $\Delta f_{\mathrm{sc}} = B/N$ where B is the bandwidth. Hence, we assume no inter-carrier interference exists for the processing at the receiver side.

A. SISO Interference Alignment with Perfect CSI

We review the concept of IA using the results in [1]. Let us assume that each transmitter and receiver has perfect CSI. Each transmitter i sends a linear combination of d_i symbols along the precoding vectors $\mathbf{v}_i^k$, yielding

$$\mathbf{x}_i[t] = \sum_{k=1}^{d_i} \mathbf{v}_i^k[t] s_i^k[t]\,, \qquad (2)$$

where $s_i^k[t] \in \mathbb{C}$ denotes the transmitted symbols and $\mathbb{E}\{\left|s_i^k[t]\right|^2\} = PN/d_i$. The precoding vector $\mathbf{v}_i^k[t]$ fulfills $\left\|\mathbf{v}_i^k[t]\right\|^2 = 1$. According to [1], each transmitter computes the precoding vectors $\mathbf{v}_i^k[t]$ such that the interference signals from the undesired $K-1$ transmitters are aligned at all receivers leaving the interference free subspace for the intended signal. Each receiver i computes the postfiltering vectors $\mathbf{u}_i^k[t]$, such that the following IA conditions are satisfied

$$\mathbf{u}_i^k[t]^{\mathrm{H}}\mathbf{W}_{i,i}[t]\mathbf{v}_i^\ell[t] = 0, \quad \forall i,\ \forall k \neq l \qquad (3)$$

$$\mathbf{u}_i^k[t]^{\mathrm{H}}\mathbf{W}_{i,j}[t]\mathbf{v}_j^\ell[t] = 0, \quad \forall i \neq j,\ \forall k,\ l \qquad (4)$$

$$\left|\mathbf{u}_i^k[t]^{\mathrm{H}}\mathbf{W}_{i,i}[t]\mathbf{v}_i^k[t]\right| \geq c > 0, \quad \forall i,\ k \qquad (5)$$

where $\mathbf{u}_i^k[t] \in \mathbb{C}^{N\times 1}$ and $\left\|\mathbf{u}_i^k[t]\right\|^2 = 1$. The achievable sum rate is given by

$$R_{\mathrm{sum}} = \sum_{i,k} \frac{1}{N} \cdot \log_2\left(1 + \frac{\frac{NP}{d_i}\left|\mathbf{u}_i^k[t]^{\mathrm{H}}\mathbf{W}_{i,i}[t]\mathbf{v}_i^k[t]\right|^2}{\sum\limits_{(i,k)\neq(j,l)} \frac{NP}{d_j}\left|\mathbf{u}_i^k[t]^{\mathrm{H}}\mathbf{W}_{i,j}[t]\mathbf{v}_j^\ell[t]\right|^2 + \sigma^2}\right). \qquad (6)$$

B. Reduced-Rank Channel Estimation and Prediction

Let us denote $w^n[t]$, $n^n[t]$ and $x^n[t]$ as the n-th element of the vector $\mathbf{w}[t]$ $\mathbf{n}[t]$ and $\mathbf{x}[t]$, respectively. The channel samples of the n-th subcarrier over time can be written as $\mathbf{g}^n = [w^n[0], \ldots, w^n[M-1]]^{\mathrm{T}}$, where M is the length of a single block. The authors of [5] and [6] show that the channel $\mathbf{g}^n$ can be approximated by a reduced rank representation which expands $\mathbf{g}^n$ by D orthonormal basis functions $\mathbf{u}_p = [u_p[0], \ldots, u_p[M-1]]^{\mathrm{T}}$, $p \in \{0, \ldots, D-1\}$

$$\mathbf{g}^n \approx \mathbf{U}\boldsymbol{\phi}^n = \sum_{p=0}^{D-1} \phi_p^n \mathbf{u}_p\,, \qquad (7)$$

where $\mathbf{U} = [\mathbf{u}_0, \ldots, \mathbf{u}_{D-1}]$ collects the basis vectors and $\boldsymbol{\phi}^n = [\phi_0^n, \ldots, \phi_{D-1}^n]$ contains the subspace coefficients for the channel $\mathbf{g}^n$.

Pilot information allows us to acquire channel knowledge. The noisy channel observations for $t \in \mathcal{P}$ is obtained as $w'^n[t] = w^n[t] + n'^n[t]$, where $\mathcal{P}$ denotes the pilot pattern and $n'^n[t] = n^n[t]x^n[t]^*$ has the same statistical properties as $n^n[t]$. Let us define $\mathbf{f}[t] = [u_0[t], \ldots, u_{D-1}[t]]^{\mathrm{T}}$, which collects the values of the basis functions at time t. The estimate of $\boldsymbol{\phi}^n$ can be calculated according to

$$\tilde{\boldsymbol{\phi}}^n = \mathbf{G}^{-1} \sum_{t\in\mathcal{P}} w'^n[t]\mathbf{f}[t]^*\,, \qquad (8)$$

where $\mathbf{G} = \sum_{t\in\mathcal{P}} \mathbf{f}[t]\mathbf{f}[t]^{\mathrm{H}}$. In this work, we use the channel prediction method presented in [5], which employs index-limited DPS sequences [7] to form the orthogonal basis vectors $\mathbf{u}_p$. The band-limiting region of the DPS sequences $\mathbf{u}_p[\mathcal{W}]$ is chosen according to the support $\mathcal{W}$ of the Doppler spectrum of the time-selective fading process, where $\mathcal{W} = (-\nu_{\mathrm{D}}, \nu_{\mathrm{D}})$ with $\nu_{\mathrm{D}} < 1/2$. To ease notation, we drop $\mathcal{W}$ in the rest of the paper. Given $\mathbf{u}_p$, [5, Sec. 3.D] shows that the sequences can be extended over $\mathbb{Z}$ in the minimum-energy band-limited sense. Thus, the predicted n-th subchannel at time instant $t \in \mathbb{Z}$ is given by

$$\tilde{w}^n[t] = \sum_{p=0}^{D-1} \tilde{\phi}_p^n u_p[t] = \mathbf{f}[t]^{\mathrm{T}}\tilde{\boldsymbol{\phi}}^n. \qquad (9)$$

The energy of the DPS sequences is most concentrated in the interval of block length M, which is defined as

$$\lambda_p = \frac{\sum\limits_{t=0}^{M-1} \left|u_p[t]\right|^2}{\sum\limits_{t=-\infty}^{\infty} \left|u_p[t]\right|^2}\,, \qquad (10)$$

where λ_p is a measure of energy concentration given the support $\mathcal{W}$ of the Doppler spectrum. The values λ_p are clustered near 1 for $p \leq \lceil 2\nu_{\mathrm{D}}M\rceil$ and decay rapidly for $p > \lceil 2\nu_{\mathrm{D}}M\rceil$. The optimal subspace dimension that minimizes the mean square error (MSE) for a given noise level is found to be [5]

$$\mathcal{D}_{\text{ub}} = \underset{D\in\{1,\ldots,M\}}{\arg\min} \left(\frac{1}{|\mathcal{W}|\,M} \sum_{p=D}^{M-1} \lambda_p + \frac{D\sigma^2}{MP} \right). \quad (11)$$

Later on we will see that $\mathcal{D}_{\text{ub}}$ is the upper bound of the subspace dimension when quantized feedback is used.

C. Channel Prediction Error

The MSE per sample is the sum of a square bias and a variance term [5]

$$\text{MSE}[t,D] = \text{bias}^2[t,D] + \text{var}[t,D] \quad (12)$$

where the variance can be approximated by $\text{var}[t,D] = \mathbf{f}[m]^{\text{T}}\mathbf{G}^{-1}\mathbf{f}[m]$. The square bias term is calculated as [5]

$$\text{bias}^2[t,D] = \int_{-\frac{1}{2}}^{\frac{1}{2}} \left| 1 - \mathbf{f}[t]^{\text{T}}\mathbf{G}^{-1} \sum_{\ell\in\mathcal{P}} \mathbf{f}[\ell] e^{-j2\pi\nu(t-\ell)} \right|^2 S_h(\nu)\mathrm{d}\nu \quad (13)$$

where $S_h(\nu)$ denotes the power spectral density of the fading process.

D. Equivalent Delay Domain Representation

We assume the N narrowband channels from the same transmitter receiver pair have the same Doppler bandwidth, thus all N fading processes share the same set of basis expansion functions. Due to the fact that $N > L$, the impulse response $\mathbf{h}[t]$ contains much less coefficients than the frequency response $\mathbf{w}[t]$. Thus, $\mathbf{h}[t]$ is better suited for CSI feedback. The equivalent basis expansion model in the delay domain can be expressed as $\left[\tilde{\mathbf{h}}[t]^{\text{T}}, \mathbf{0}_{1\times(N-L)}\right]^{\text{T}} = [\tilde{\boldsymbol{\gamma}}^1, \ldots, \tilde{\boldsymbol{\gamma}}^L, \mathbf{0}_{D\times(N-L)}]^{\text{T}}\mathbf{f}[t]$, where

$$\begin{aligned} &[\tilde{\boldsymbol{\gamma}}^1, \ldots, \tilde{\boldsymbol{\gamma}}^L, \mathbf{0}_{D\times(N-L)}]^{\text{T}} \\ &= \begin{bmatrix} \sqrt{N}\mathcal{F}_N^{-1}\left\{\left[\tilde{\phi}_0^1, \ldots, \tilde{\phi}_0^N\right]\right\} \\ \vdots \\ \sqrt{N}\mathcal{F}_N^{-1}\left\{\left[\tilde{\phi}_{D-1}^1, \ldots, \tilde{\phi}_{D-1}^N\right]\right\} \end{bmatrix}^{\text{T}} \end{aligned} \quad (14)$$

is obtained due to the linearity of the Fourier transform and $\tilde{\boldsymbol{\gamma}}^\ell$ is the vector containing the basis expansion coefficients corresponding to the ℓ-th channel tap $\tilde{h}^l[t]$. We use these delay domain coefficients $\tilde{\boldsymbol{\gamma}}^\ell$ to build up the limited feedback systems.

E. Reformulation of Subspace Representation for the SISO Interference Channels

With the subspace coefficients $\tilde{\boldsymbol{\gamma}}^\ell$ obtained from (14), the predicted channel impulse response can be written as

$$\begin{aligned} \tilde{\mathbf{h}}[t] &= [\tilde{\boldsymbol{\gamma}}^1, \ldots, \tilde{\boldsymbol{\gamma}}^L]^{\text{T}}\mathbf{f}[t] \\ &= \underbrace{\begin{bmatrix} \mathbf{f}[t]^{\text{T}} & \mathbf{0}_D^{\text{T}} & \ldots & \mathbf{0}_D^{\text{T}} \\ \mathbf{0}_D^{\text{T}} & \mathbf{f}[t]^{\text{T}} & \ldots & \mathbf{0}_D^{\text{T}} \\ \vdots & \vdots & \ddots & \vdots \\ \mathbf{0}_D^{\text{T}} & \mathbf{0}_D^{\text{T}} & \ldots & \mathbf{f}[t]^{\text{T}} \end{bmatrix}}_{\mathbf{F}[t]} \underbrace{\begin{bmatrix} \tilde{\boldsymbol{\gamma}}^1 \\ \vdots \\ \tilde{\boldsymbol{\gamma}}^L \end{bmatrix}}_{\tilde{\boldsymbol{\eta}}}, \end{aligned} \quad (15)$$

where $\tilde{\boldsymbol{\eta}} \in \mathbb{C}^{DL\times 1}$ and $\mathbf{F} \in \mathbb{C}^{L\times DL}$.

In the next section, we will show that the achievable rate for IA is invariant to a norm change and phase rotation of $\tilde{\boldsymbol{\eta}}$. Therefore, it is equivalent to know $\tilde{\boldsymbol{\eta}}$ or $\alpha\tilde{\boldsymbol{\eta}}$ at the transmitter side, where $\alpha \in \mathbb{C}$. Thus, the CSI feedback problem becomes feeding back a point on the Grassmannian manifold $\mathcal{G}_{DL,1}$.

III. Time-variant Channel Quantization for IA

In this section, we consider a limited feedback scheme for subspace coefficients $\tilde{\boldsymbol{\eta}}_{i,j}$. We prefer to feed back $\tilde{\boldsymbol{\eta}}_{i,j}$ since it enables channel prediction at the transmitter side, which is extremely useful for a delayed feedback system. Figure 1 shows the working principle of the feedback system. The subspace coefficients are estimated from the training phase and fed back via a feedback channel with delay. Each receiver estimates the channels to all K transmitters separately. To this end, the pilot symbols from different transmitters are orthogonalized in time. The number of pilot symbols for each transmitter is M/K.

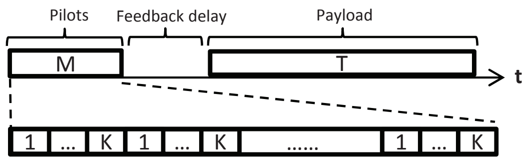

Fig. 1. Signaling model, where M denotes the length of the pilot sequence and T the payload length.

A. SISO Interference Alignment with Imperfect CSI

Imperfect CSI results in residual interference, thus, IA conditions (3) and (4) can not be satisfied. Let us define the average loss in sum rate as $\Delta R = \mathbb{E}[R_{\text{sum}}^{\text{perfect}}] - \mathbb{E}[R_{\text{sum}}]$, where $R_{\text{sum}}^{\text{perfect}}$ is the sum rate achieved with perfect CSI and the vectors in (3)-(5), and R_{sum} is the sum rate given imperfect precoding vectors $\hat{\mathbf{v}}_i^k[t]$ and postfiltering vectors $\hat{\mathbf{u}}_i^k[t]$. An upper bound of the average loss in sum rate ΔR is given by [8]

$$\Delta R < \sum_{i,k} \frac{1}{N} \log_2 \left(1 + \frac{\mathbb{E}\left[\mathcal{I}_i^k\right]}{\sigma^2} \right), \quad (16)$$

where

$$\mathcal{I}_i^k = \sum_{(i,k)\neq(j,\ell)} \frac{NP}{d_j} \left| \hat{\mathbf{u}}_i^k[t]^{\text{H}} \mathbf{W}_{i,j}[t] \hat{\mathbf{v}}_j^\ell[t] \right|^2 \quad (17)$$

denotes the sum of inter-stream interference and inter-user interference.

B. CSI Quantization and Achievable Rate Analysis

We define $\hat{\mathbf{b}}_{i,j}^{k,\ell}[t] = \hat{\mathbf{u}}_i^k[t] \circ \hat{\mathbf{v}}_j^\ell[t]$ as the Hadamard product of the postfiltering vector $\hat{\mathbf{u}}_i^k[t]$ and precoding vector $\hat{\mathbf{v}}_j^\ell[t]$. The leakage interference in (17) can be rewritten as

$$\mathcal{I}_i^k = \sum_{(i,k)\neq(j,\ell)} \frac{NP}{d_j} \left| \mathbf{w}_{i,j}[t]^{\text{H}} \hat{\mathbf{b}}_{i,j}^{k,\ell}[t] \right|^2. \quad (18)$$

We define the predicted channel frequency response $\tilde{\mathbf{w}}_{i,j}[t] = [\tilde{w}^1_{i,j}[t], \ldots, \tilde{w}^n_{i,j}[t]]^{\mathrm{T}}$ and the prediction error $\tilde{\mathbf{z}}_{i,j}[t]^{\mathrm{H}} = \mathbf{w}_{i,j}[t] - \tilde{\mathbf{w}}_{i,j}[t]$. The average power of leakage interference in (16) can be upper bounded by

$$\mathbb{E}[\mathcal{I}_{i,k}]$$

$$= \sum_{(i,k)\neq(j,\ell)} \frac{NP}{d_i}\mathbb{E}\left[\left|\mathbf{w}_{i,j}[t]^{\mathrm{H}}\hat{\mathbf{b}}^{k,\ell}_{i,j}[t]\right|^2\right] \tag{19}$$

$$= \sum_{(i,k)\neq(j,\ell)} \frac{NP}{d_i}\mathbb{E}\left[\left|\left(\tilde{\mathbf{w}}_{i,j}[t]^{\mathrm{H}} + \tilde{\mathbf{z}}_{i,j}[t]^{\mathrm{H}}\right)\hat{\mathbf{b}}^{k,\ell}_{i,j}[t]\right|^2\right] \tag{20}$$

$$= \sum_{(i,k)\neq(j,\ell)} \frac{NP}{d_i}\Bigg(\mathbb{E}\Bigg[\left|\tilde{\mathbf{w}}_{i,j}[t]^{\mathrm{H}}\hat{\mathbf{b}}^{k,\ell}_{i,j}[t]\right|^2 + \left|\tilde{\mathbf{z}}_{i,j}[t]^{\mathrm{H}}\hat{\mathbf{b}}^{k,\ell}_{i,j}[t]\right|^2$$

$$+ 2\mathrm{Re}\left(\tilde{\mathbf{w}}_{i,j}[t]^{\mathrm{H}}\hat{\mathbf{b}}^{k,\ell}_{i,j}[t]\hat{\mathbf{b}}^{k,\ell}_{i,j}[t]^{\mathrm{H}}\tilde{\mathbf{z}}_{i,j}[t]\right)\Bigg]\Bigg) \tag{21}$$

$$= \sum_{(i,k)\neq(j,\ell)} \Bigg(\underbrace{\frac{NP}{d_i}\mathbb{E}\left[\left|\tilde{\mathbf{z}}_{i,j}[t]^{\mathrm{H}}\hat{\mathbf{b}}^{k,\ell}_{i,j}[t]\right|^2\right]}_{\tilde{\Delta}^{k,\ell}_{i,j}[t]} +$$

$$\underbrace{\frac{NP}{d_i}\mathbb{E}\left[\left|\tilde{\mathbf{w}}_{i,j}[t]^{\mathrm{H}}\hat{\mathbf{b}}^{k,\ell}_{i,j}[t]\right|^2\right]}_{\hat{\Delta}^{k,\ell}_{i,j}[t]}\Bigg) \tag{22}$$

where (22) is obtained due to the fact that the prediction error $\tilde{\mathbf{z}}_{i,j}[t]$ is independent of the channel frequency response $\tilde{\mathbf{w}}_{i,j}[t]$, i.e. $\mathbb{E}\left[\mathrm{Re}\left(\tilde{\mathbf{w}}_{i,j}[t]^{\mathrm{H}}\hat{\mathbf{b}}^{k,\ell}_{i,j}[t]\hat{\mathbf{b}}^{k,\ell}_{i,j}[t]^{\mathrm{H}}\tilde{\mathbf{z}}_{i,j}[t]\right)\right] = 0$. The first and second term in (22) is caused by the channel prediction error and the quantization error respectively.

The first term $\tilde{\Delta}^{k,\ell}_{i,j}[t]$ in (22) can be written as

$$\tilde{\Delta}^{k,\ell}_{i,j}[t] = \frac{NP}{d_i}\mathbb{E}\left[\left|\tilde{\mathbf{z}}_{i,j}[t]^{\mathrm{H}}\hat{\mathbf{b}}^{k,\ell}_{i,j}[t]\right|^2\right]$$

$$= \frac{P}{d_i}\mathbb{E}\|\hat{\mathbf{b}}^{k,\ell}_{i,j}[t]\|^2\mathbb{E}\,\|\tilde{\mathbf{z}}_{i,j}[t]\|^2 \tag{23}$$

$$= \frac{P}{d_i}\mathbb{E}\|\hat{\mathbf{b}}^{k,\ell}_{i,j}[t]\|^2\sum_{n=1}^{N}\mathbb{E}\left|\tilde{z}^n_{i,j}[t]\right|^2 \tag{24}$$

$$= \frac{P}{d_i}\mathrm{MSE}[t, D]\ , \tag{25}$$

where (23) follows from the fact that $\hat{\mathbf{b}}^{k,\ell}_{i,j}[t]$ and $\tilde{\mathbf{z}}_{i,j}[t]$ are independent and all the elements of each vector have the same statistical properties. Equation (25) is obtained using the results from (12) and $\mathbb{E}\|\hat{\mathbf{b}}^{k,\ell}_{i,j}[t]\|^2 = 1/N$.

Defining $\sqrt{N}\mathcal{F}_N^{-1}\{\hat{\mathbf{b}}^{k,\ell}_{i,j}[t]\} = [\hat{\mathbf{q}}^{k,\ell}_{i,j}[t]^{\mathrm{T}}, \mathbf{q}^{k,\ell}_{i,j}[t]^{\mathrm{T}}]^{\mathrm{T}}$, where $\hat{\mathbf{q}}^{k,\ell}_{i,j}[t] \in \mathbb{C}^{L\times 1}$ and $\mathbf{q}^{k,\ell}_{i,j}[t] \in \mathbb{C}^{(N-L)\times 1}$, the second term $\hat{\Delta}^{k,\ell}_{i,j}[t]$ in (22) can be rewritten as

$$\hat{\Delta}^{k,\ell}_{i,j}[t] = \frac{NP}{d_i}\mathbb{E}\left[\left|\tilde{\mathbf{w}}_{i,j}[t]^{\mathrm{H}}\hat{\mathbf{b}}^{k,\ell}_{i,j}[t]\right|^2\right]$$

$$= \frac{NP}{d_i}\mathbb{E}\left[\left|\tilde{\mathbf{h}}_{i,j}[t]^{\mathrm{H}}\hat{\mathbf{q}}^{k,\ell}_{i,j}[t]\right|^2\right] \tag{26}$$

$$= \frac{NP}{d_i}\mathbb{E}\left[\left|\tilde{\boldsymbol{\eta}}^{\mathrm{H}}_{i,j}\mathbf{F}_{i,j}[t]^{\mathrm{H}}\hat{\mathbf{q}}^{k,\ell}_{i,j}[t]\right|^2\right]. \tag{27}$$

Let us define $\hat{\boldsymbol{\eta}}_{i,j}$ as the quantized version of $\tilde{\boldsymbol{\eta}}_{i,j}$ and $\|\hat{\boldsymbol{\eta}}_{i,j}\| = 1$. From Parseval's theorem we have $\hat{\mathbf{q}}^{k,\ell}_{i,j}[t]^{\mathrm{H}}\mathbf{F}_{i,j}[t]\hat{\boldsymbol{\eta}}_{i,j} = 0$. We can define an orthonormal basis in $\mathbb{C}^{DL}$ as

$$\left\{\hat{\boldsymbol{\eta}}_{i,j}, \frac{\mathbf{F}_{i,j}[t]^{\mathrm{H}}\hat{\mathbf{q}}^{k,\ell}_{i,j}[t]}{\|\mathbf{F}_{i,j}[t]^{\mathrm{H}}\hat{\mathbf{q}}^{k,\ell}_{i,j}[t]\|}, \mathbf{d}_1, \mathbf{d}_2, \ldots, \mathbf{d}_{DL-2}\right\}, \tag{28}$$

where $[\mathbf{d}_1, \mathbf{d}_2, \ldots, \mathbf{d}_{DL-2}]$ is an orthonormal basis of $\mathrm{null}([\hat{\boldsymbol{\eta}}_{i,j}, \frac{\mathbf{F}_{i,j}[t]^{\mathrm{H}}\hat{\mathbf{q}}^{k,\ell}_{i,j}[t]}{\|\mathbf{F}_{i,j}[t]^{\mathrm{H}}\hat{\mathbf{q}}^{k,\ell}_{i,j}[t]\|}]^{\mathrm{H}})$. We can decompose $\tilde{\boldsymbol{\eta}}_{i,j}$ into the above orthonormal basis, i.e.

$$\|\tilde{\boldsymbol{\eta}}_{i,j}\|^2 \tag{29}$$

$$= \left|\hat{\boldsymbol{\eta}}^{\mathrm{H}}_{i,j}\tilde{\boldsymbol{\eta}}_{i,j}\right|^2 + \left|\frac{\hat{\mathbf{q}}^{k,\ell}_{i,j}[t]^{\mathrm{H}}\mathbf{F}_{i,j}[t]^{\mathrm{H}}}{\|\mathbf{F}_{i,j}[t]^{\mathrm{H}}\hat{\mathbf{q}}^{k,\ell}_{i,j}[t]\|}\tilde{\boldsymbol{\eta}}_{i,j}\right|^2 + \sum_{m=1}^{DL-2}\left|\mathbf{d}^{\mathrm{H}}_m\tilde{\boldsymbol{\eta}}_{i,j}\right|^2. \tag{30}$$

Inserting (30) into (27) yields

$$\frac{NP}{d_i}\mathbb{E}\left[\left|\tilde{\boldsymbol{\eta}}^{\mathrm{H}}_{i,j}\mathbf{F}_{i,j}[t]^{\mathrm{H}}\hat{\mathbf{q}}^{k,\ell}_{i,j}[t]\right|^2\right] \tag{31}$$

$$= \frac{NP}{d_i}\mathbb{E}\Bigg[\|\mathbf{F}_{i,j}[t]^{\mathrm{H}}\hat{\mathbf{q}}^{k,\ell}_{i,j}[t]\|^2$$

$$\left(\|\tilde{\boldsymbol{\eta}}_{i,j}\|^2 - |\hat{\boldsymbol{\eta}}^{\mathrm{H}}_{i,j}\tilde{\boldsymbol{\eta}}_{i,j}|^2 - \sum_{m=1}^{DL-2}\left|\mathbf{d}^{\mathrm{H}}_m\tilde{\boldsymbol{\eta}}_{i,j}\right|^2\right)\Bigg] \tag{32}$$

$$= \frac{NP}{d_i(DL-1)}\mathbb{E}\|\mathbf{F}_{i,j}[t]^{\mathrm{H}}\hat{\mathbf{q}}^{k,\ell}_{i,j}[t]\|^2\mathbb{E}\left[\|\tilde{\boldsymbol{\eta}}_{i,j}\|^2 - |\hat{\boldsymbol{\eta}}^{\mathrm{H}}_{i,j}\tilde{\boldsymbol{\eta}}_{i,j}|^2\right] \tag{33}$$

$$= \frac{NP}{d_i(DL-1)}\mathbb{E}\|\mathbf{F}_{i,j}[t]^{\mathrm{H}}\hat{\mathbf{q}}^{k,\ell}_{i,j}[t]\|^2\mathbb{E}\|\tilde{\boldsymbol{\eta}}_{i,j}\|^2\mathbb{E}\left[d^2_{\mathrm{c}}\left(\frac{\tilde{\boldsymbol{\eta}}_{i,j}}{\|\tilde{\boldsymbol{\eta}}_{i,j}\|}, \hat{\boldsymbol{\eta}}_{i,j}\right)\right] \tag{34}$$

where $d_{\mathrm{c}}(\mathbf{x}_1, \mathbf{x}_2) = \sqrt{(1 - |\mathbf{x}^{\mathrm{H}}_1\mathbf{x}_2|^2)}$ is the chordal distance between two unit norm vectors $\mathbf{x}_1$ and $\mathbf{x}_2$. Equation (33) follows from the fact that the average power of $\tilde{\boldsymbol{\eta}}_{i,j}$ in each dimension of $\left\{\frac{\mathbf{F}_{i,j}[t]^{\mathrm{H}}\hat{\mathbf{q}}^{k,\ell}_{i,j}[t]}{\|\mathbf{F}_{i,j}[t]^{\mathrm{H}}\hat{\mathbf{q}}^{k,\ell}_{i,j}[t]\|}, \mathbf{d}_1, \mathbf{d}_2, \ldots, \mathbf{d}_{DL-2}\right\}$ is equal. Equation (34) follows from the independence of the norm and the angle of $\tilde{\boldsymbol{\eta}}_{i,j}$.

Equation (34) shows that the leakage interference can be bounded by the chordal distance between the true and the quantized subspace coefficients. The optimal codebook for quantization can be generated numerically using the Grassmannian line-packing approach. However, it is challenging to find the optimal codewords which achieve the quantization bound promised by [9], except for some specific cases.

In our work, random vector quantization (RVQ) codebooks are used. The term $Q(N_{\mathrm{d}}) = \mathbb{E}\left[d^2_{\mathrm{c}}\left(\frac{\tilde{\boldsymbol{\eta}}_{i,j}}{\|\tilde{\boldsymbol{\eta}}_{i,j}\|}, \hat{\boldsymbol{\eta}}_{i,j}\right)\right]$ is the expectation of the quantization error. As shown in [9], for quantizing a vector arbitrarily distributed on the Grassmannian manifold $\mathcal{G}_{DL,1}$, the second moment of the chordal distance using N_{d} quantization bits can be bounded as

$$Q(N_{\mathrm{d}}) \leq \frac{\Gamma(\frac{1}{DL-1})}{DL-1}(c2^{N_{\mathrm{d}}})^{-\frac{1}{DL-1}}\ , \tag{35}$$

where $\Gamma(\cdot)$ denotes the Gamma function.

Furthermore, we have $\mathbb{E}\|\mathbf{F}_{i,j}[t]^{\mathrm{H}}\hat{\mathbf{q}}_{i,j}^{k,\ell}[t]\|^2 = \frac{\|\mathbf{F}_{i,j}[t]\|_{\mathrm{F}}^2}{N^2}$ and $\mathbb{E}\|\tilde{\boldsymbol{\eta}}_{i,j}\|^2 = \mathrm{tr}(\mathbf{U}^{\mathrm{H}}(\mathbf{R}_{\mathrm{h}}+\sigma_{\mathrm{n}}^2\mathbf{I}_{\mathrm{L}})\mathbf{U})$, where $\mathbf{R}_{\mathbf{h}_{i,j}}$ is the temporal covariance matrix with elements $[\mathbf{R}_{\mathbf{h}_{i,j}}]_{l,m} = R_{\mathbf{h}_{i,j}}[l-m]$ for $l,m \in [0,\ldots,M-1]$ and $\mathrm{tr}(\mathbf{A})$ denotes the trace of matrix $\mathbf{A}$. Plugging in the above results, (34) can be further bounded as

$$\begin{aligned}&\frac{NP}{d_i}\mathbb{E}\left[\left|\tilde{\boldsymbol{\eta}}_{i,j}^{\mathrm{H}}\mathbf{F}_{i,j}[t]^{\mathrm{H}}\hat{\mathbf{q}}_{i,j}^{k,\ell}[t]\right|^2\right]\\ &\leq \frac{P\|\mathbf{F}_{i,j}[t]\|_{\mathrm{F}}^2}{d_iN(DL-1)}\mathrm{tr}\left(\mathbf{U}^{\mathrm{H}}\left(\mathbf{R}_h+\sigma_n^2\mathbf{I}_L\right)\mathbf{U}\right)Q(N_{\mathrm{d}}). \qquad (36)\end{aligned}$$

In order to bound the interference leakage power such that it is a constant when $P \longrightarrow \infty$, we need to make (36) independent of P. This implies

$$Q(N_{\mathrm{d}}) \propto \frac{1}{P} \Rightarrow N_{\mathrm{d}} = (DL-1)\log_2 kP, \qquad (37)$$

where $k > 0$ is a constant. If N_d grows as shown in (37), the rate loss due to quantization error is a constant. The average rate loss due to channel prediction and quantization can be upper bound by

$$\Delta R < \frac{1}{NT}\sum_{t\in\mathcal{T}}\sum_{i,k}\log_2\left(1+\frac{\sum\limits_{(i,k)\neq(j,l)}\left(\tilde{\Delta}_{i,j}^{k,\ell}[t]+\hat{\Delta}_{i,j}^{k,\ell}[t]\right)}{\sigma^2}\right) \qquad (38)$$

When the subspace coefficients are unquantized, the optimal subspace dimension that minimizes the prediction error is given in equation (11). However, a limited feedback system exhibits a tradeoff between the quality of channel prediction and quantization. For $\mathcal{D}_{\mathrm{ub}} > 1$, an *adaptive subspace dimension switching* algorithm is proposed, which finds the optimal subspace dimension analytically by evaluating (38), i.e.

$$\mathcal{D}_{\mathrm{opt}} = \underset{D\in\{1,\ldots,\mathcal{D}_{\mathrm{ub}}\}}{\arg\min}\ \Delta R. \qquad (39)$$

IV. Simulation Results

In this section, the sum rate of the proposed scheme is evaluated through Monte-Carlo simulations using the precoders and post-filters obtained by the closed-form IA algorithm [1] over $N = 3$ channel extensions. We consider a $K = 3$ user interference channel, where each channel has L delay taps and a flat power delay profile i.e. $\mathbb{E}\{\mathbf{h}_{i,j}[t]\mathbf{h}_{i,j}[t]^{\mathrm{H}}\} = \mathbf{I}_L/L$. Each delay tap $h_{i,j}{}^{\ell}[t]$ is temporally correlated according to Clarke's model [10]. The OFDM symbol rate $1/T_s = 1.4\times10^4$Hz is chosen according to the 3GPP LTE standard [11]. The carrier frequency is $f_c = 2.5$GHz. In order to enable the performance analysis with exponentially large codebooks, we replace the RVQ process by the statistical model of the quantization error using random perturbations [12, Sec. VI.B], which has shown to be a good approximation of the quantization error using RVQ.

Fig. 2 illustrates the sum rate with different number of feedback bits versus SNR for $\nu_{\mathrm{D}} = 0.002$ (12.1km/h). The

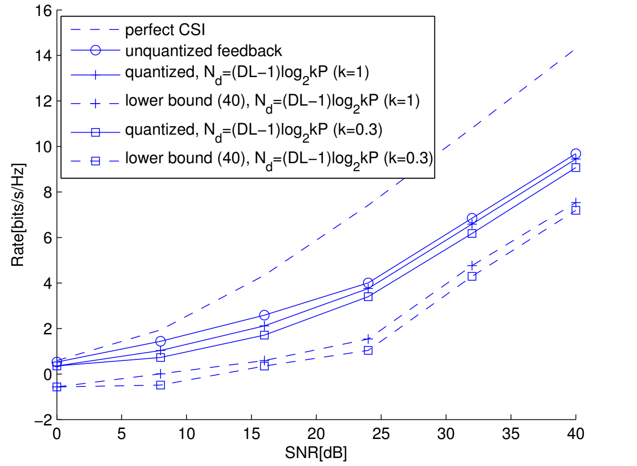

Fig. 2. Sum rate versus SNR at normalized Doppler frequency $\nu_{\mathrm{D}} = 0.002$. The length of the pilot sequence $M = 15$. The length of the payload $T = 45$. The number of channel taps $L = 3$.

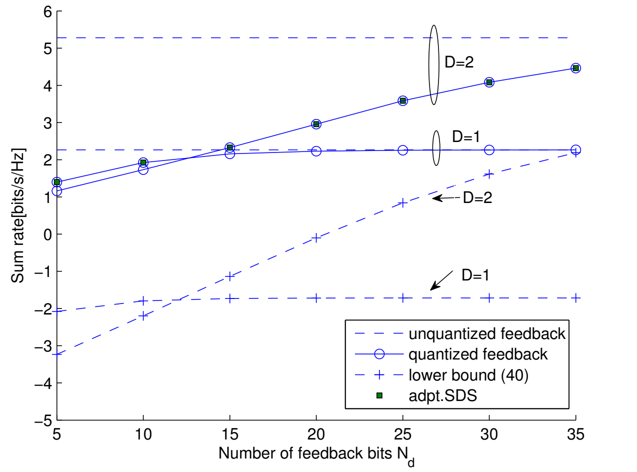

Fig. 3. Sum rate versus the number of feedback bits at SNR=30dB and the normalized Doppler frequency $\nu_{\mathrm{D}} = 0.004$. The length of the pilot sequence $M = 15$. The length of the payload $T = 45$. The number of channel taps $L = 3$.

number of feedback bits is scaled according to (37). Compared to unquantized feedback, the rate loss due to quantization remains constant with the increase of SNR. With different constant k, the curves achieve the same slope at high SNRs. It implies that the scaling law of (37) is efficient to preserve the DoF achieved by the unquantized feedback. The rate loss at high SNRs is caused by the channel prediction error. The lower bound of the average achievable rate is derived as

$$R_{\mathrm{lb}} = \mathbb{E}\left[R_{\mathrm{sum}}^{\mathrm{perfect}}\right] - \Delta R. \qquad (40)$$

Fig. 3 shows the sum rate versus the number of feedback bits at SNR=30dB and the normalized Doppler frequency $\nu_D = 0.004$ (24.2km/h). For such a setting, equation (11) suggests that the optimal subspace dimension $\mathcal{D}_{\mathrm{ub}}$ is 2 for unquantized feedback. However, as discussed earlier, higher

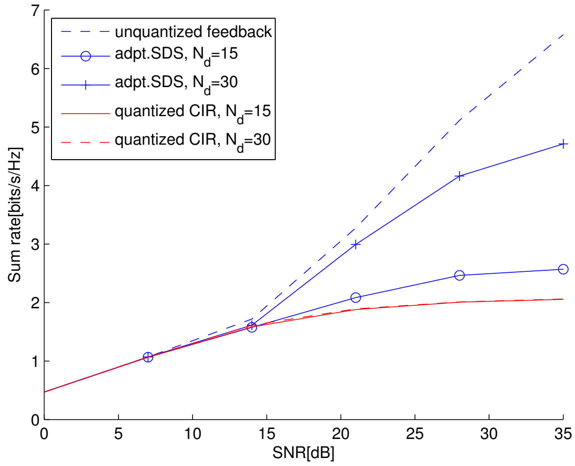

Fig. 4. Sum rate versus SNR at normalized Doppler frequency $\nu_{\mathrm{D}} = 0.004$. A 0.5 ms feedback delay $T_{\mathrm{D}} = 7$ is considered $\forall i, j$. The length of the pilot sequence $M = 15$. The length of the payload $T = 30$. The number of channel taps $L = 3$.

subspace dimension might lead to a larger quantization error. To find the best subspace dimension, we present the achieved rate and the corresponding lower bound at both $D = \{1, 2\}$. It can be observed that the achieved sum rate increases with the number of feedback bits. For $D = 1$, it achieves an initial higher rate due to smaller quantization error. The achieved rate becomes a constant with the increase of N_d due to the dominance of the prediction error. When more than 15 bits are used, the two dimensional subspace outperforms the one dimensional subspace due to the better capability of channel prediction. The tradeoff between the quality of channel prediction and quantization is well captured by the lower bounds, which exhibit almost the same switching point as that obtained by simulation. Thus, the adaptive subspace dimension switching algorithm (39), denoted as adpt.SDS, is efficient to find the subspace dimension associated with a higher rate.

Fig. 4 illustrates the sum rate at normalized Doppler frequency $\nu_{\mathrm{D}} = 0.004$ (24.2km/h) with feedback delay $T_{\mathrm{D}} = 7$ (0.5 ms) $\forall i, j$. The performance is compared to the traditional non-predictive strategy (denoted as "quantized CIR" in Fig. 4), which feeds back the channel impulse response (CIR) and assumes the channel is constant over a frame length. The estimate of the impulse response is obtained using the solution presented in Sec. II-B and then averaged over all pilot positions. It can be observed that feeding back only quantized CIR achieves a low rate due to outdated CSI. The prediction algorithm with adapt.SDS has a subspace dimension $D = 1$ at low SNRs, which results in a similar performance to "quantized CIR". For SNR> 13dB, the optimal subspace dimension D becomes 2. As a result, better channel prediction is achieved at high SNR, especially for a large number of feedback bits. The adaptive subspace dimension switching algorithm is able to efficiently find the dimension associated with a higher rate, which guarantees the superiority of the proposed feedback scheme over the non-predictive strategy.

V. Conclusion

We proposed a novel limited feedback algorithm for SISO interference alignment. The feedback algorithm enables reduced-rank channel prediction, which reduces the channel estimation error due to user mobility and feedback delay. We characterized the scaling of the required number of bits in order to decouple the rate loss due to channel quantization from the transmit power. We derived an upper bound of the rate loss due to channel prediction and quantization error, which was used to facilitate an adaptive subspace dimension switching algorithm. The algorithm is efficient to find the best tradeoff between prediction error and quantization error. Simulation results showed that a rate gain over the non-predictive strategy can be obtained.

Acknowledgment

This work was supported by the project NFN SISE (S10607) funded by the Austrian Science Fund (FWF) as well as the FTW strategic project I-0. The Austrian Competence Center "FTW Forschungszentrum Telekommunikation Wien GmbH" is funded within the program COMET - Competence Centers for Excellent Technologies by BMVIT, BMWFJ, and the City of Vienna. The COMET program is managed by the FFG.

References

[1] V. Cadambe and S. Jafar, "Interference alignment and degrees of freedom of the K-user interference channel," *IEEE Trans. Inf. Theory*, vol. 54, no. 8, pp. 3425 –3441, August 2008.

[2] D. J. Love, R. W. Heath, V. K. Lau, D. Gesbert, B. D. Rao, and M. Andrews, "An overview of limited feedback in wireless communication systems," *IEEE J. Sel. Areas Commun.*, vol. 26, no. 8, pp. 1341–1365, 2008.

[3] H. Bölcskei and I. Thukral, "Interference alignment with limited feedback," in *Proc. International Symposium on Information Theory*, 2009, pp. 1759–1763.

[4] R. T. Krishnamachari and M. K. Varanasi, "Interference alignment under limited feedback for MIMO interference channels," in *Proc. International Symposium on Information Theory*, 2010, pp. 619–623.

[5] T. Zemen, C. Mecklenbräuker, F. Kaltenberger, and B. H. Fleury, "Minimum-energy band-limited predictor with dynamic subspace selection for time-variant flat-fading channels," *IEEE Trans. Signal Process.*, vol. 55, no. 9, pp. 4534–4548, 2007.

[6] F. A. Dietrich and W. Utschick, "Pilot-assisted channel estimation based on second-order statistics," *IEEE Trans. Signal Process.*, vol. 53, no. 3, pp. 1178–1193, 2005.

[7] D. Slepian, "Prolate spheroidal wave functions, fourier analysis, and uncertainty—V: the discrete case," *The Bell System Technical Journal*, vol. 57, no. 5, pp. 1371–1430, 1978.

[8] O. E. Ayach and R. W. Heath, "Interference alignment with analog channel state feedback," *IEEE Trans. Wireless Commun.*, vol. 11, no. 2, pp. 626–636, 2012.

[9] W. Dai, Y. Liu, and B. Rider, "Quantization bounds on grassmann manifolds and applications to mimo communications," *Information Theory, IEEE Transactions on*, vol. 54, no. 3, pp. 1108–1123, 2008.

[10] R. H. Clarke, "A statistical theory of mobile-radio reception," *Bell System Technical Journal*, p. 957, July-August 1968.

[11] 3rd Generation Partnership Project (3GPP), *Technical Specification Group Radio Access Network; Physical layer aspects for evolved Universal Terrestrial Radio Access (UTRA) (Release 7)*, Std.

[12] M. Rezaee and M. Guillaud, "Interference alignment with quantized grassmannian feedback in the K-user constant MIMO interference channel," Jul. 2012. [Online]. Available: arXiv:1207.6902